Research Article | Vol. 25, No. 12 | 12 Jun 2017 | OPTICS EXPRESS 13351
Optics EXPRESS

Near diffraction-limited performance of an OPA pumped acetylene-filled hollow-core fiber laser in the mid-IR

NEDA DADASHZADEH,[1] MANASADEVI P. THIRUGNANASAMBANDAM,[1] H. W. KUSHAN WEERASINGHE,[1] BENOIT DEBORD,[2] MATTHIEU CHAFER,[2] FREDERIC GEROME,[2] FETAH BENABID,[2] BRIAN R. WASHBURN,[1] AND KRISTAN L. CORWIN[1,*]

[1]*Department of Physics, Kansas State University, Manhattan, KS 66506, USA*
[2]*GPPMM group, Xlim Research Institute, UMR CNRS 7252, University of Limoges, France*
**corwin@phys.ksu.edu*

Abstract: We investigate the mid-IR laser beam characteristics from an acetylene-filled hollow-core optical fiber gas laser (HOFGLAS) system. The laser exhibits near-diffraction limited beam quality in the 3 μm region with $M^2 = 1.15 \pm 0.02$ measured at high pulse energy, and the highest mid-IR pulse energy from a HOFGLAS system of 1.4 μJ is reported. Furthermore, the effects of output saturation with pump pulse energy are reduced through the use of longer fibers with low loss. Finally, the slope efficiency is shown to be nearly independent of gas pressure over a wide range, which is encouraging for further output power increase.

OCIS codes: (140.4130) Molecular gas lasers; (140.3510) Lasers, fiber; (060.5295) Photonic crystal fibers; (140.3070) Infrared and far-infrared lasers.

References and Links

1. A. A. Ionin, "Electric Discharge CO Lasers," in *Gas Lasers,* M. Endo, and R. F. Walter, ed. (Chemical Rubber Company, 2007), pp. 201–237.
2. W. F. Krupke, R. J. Beach, V. K. Kanz, and S. A. Payne, "Resonance transition 795-nm rubidium laser," Opt. Lett. **28**(23), 2336–2338 (2003).
3. B. V. Zhdanov, T. Ehrenreich, and R. J. Knize, "Highly efficient optically pumped cesium vapor laser," Opt. Commun. **260**(2), 696–698 (2006).
4. J. Zweiback, A. Komashko, and W. F. Krupke, "Alkali vapor lasers," Proc. SPIE **7581**, 75810G (2010).
5. A. V. V. Nampoothiri, A. Ratanavis, N. Campbell, and W. Rudolph, "Molecular C_2H_2 and HCN lasers pumped by an optical parametric oscillator in the 1.5-μm band," Opt. Express **18**(3), 1946–1951 (2010).
6. J. W. Dawson, M. J. Messerly, R. J. Beach, M. Y. Shverdin, E. A. Stappaerts, A. K. Sridharan, P. H. Pax, J. E. Heebner, C. W. Siders, and C. P. J. Barty, "Analysis of the scalability of diffraction-limited fiber lasers and amplifiers to high average power," Opt. Express **16**(17), 13240–13266 (2008).
7. A. M. Jones, A. V. V. Nampoothiri, A. Ratanavis, T. Fiedler, N. V. Wheeler, F. Couny, R. Kadel, F. Benabid, B. R. Washburn, K. L. Corwin, and W. Rudolph, "Mid-infrared gas filled photonic crystal fiber laser based on population inversion," Opt. Express **19**(3), 2309–2316 (2011).
8. A. V. V. Nampoothiri, A. M. Jones, A. Ratanavis, R. Kadel, N. V. Wheeler, F. Couny, F. Benabid, B. R. Washburn, K. L. Corwin, and W. Rudolph, "Mid-IR laser emission from a C_2H_2 gas filled hollow core photonic crystal fiber," Proc. SPIE **7580**, 758001 (2010).
9. A. M. Jones, C. Fourcade-Dutin, C. Mao, B. Baumgart, A. V. V. Nampoothiri, N. Campbell, Y. Wang, F. Benabid, W. Rudolph, B. R. Washburn, and K. L. Corwin, "Characterization of mid-infrared emissions from C_2H_2, CO, CO_2, and HCN-filled hollow fiber lasers," Proc. SPIE **8237**, 82373Y (2012).
10. A. Ratanavis, N. Campbell, and W. Rudolph, "Feasibility study of optically pumped molecular lasers with small quantum defect," Opt. Commun. **283**(6), 1075–1080 (2010).
11. A. V. V. Nampoothiri, A. M. Jones, C. Fourcade-Dutin, C. Mao, N. Dadashzadeh, B. Baumgart, Y. Y. Wang, M. Alharbi, T. Bradley, N. Campbell, F. Benabid, B. R. Washburn, K. L. Corwin, and W. Rudolph, "Hollow-core Optical Fiber Gas Lasers (HOFGLAS): a review [Invited]," Opt. Mater. Express **2**(7), 948–961 (2012).
12. A. V. V. Nampoothiri, B. Debord, M. Alharbi, F. Gérôme, F. Benabid, and W. Rudolph, "CW hollow-core optically pumped I_2 fiber gas laser," Opt. Lett. **40**(4), 605–608 (2015).
13. M. Abu Hassan, F. Yu, W. Wadsworth, and J. Knight, "Cavity-based mid-IR fiber gas laser pumped by a diode laser," Optica **3**(3), 218–221 (2016).

#287880 https://doi.org/10.1364/OE.25.013351
Journal © 2017 Received 24 Mar 2017; revised 15 May 2017; accepted 16 May 2017; published 2 Jun 2017

Optics EXPRESS

14. F. Benabid, J. C. Knight, G. Antonopoulos, and P. S. J. Russell, "Stimulated Raman scattering in hydrogen-filled hollow-core photonic crystal fiber," Science **298**(5592), 399–402 (2002).
15. F. Couny, F. Benabid, P. J. Roberts, P. S. Light, and M. G. Raymer, "Generation and photonic guidance of multi-octave optical-frequency combs," Science **318**(5853), 1118–1121 (2007).
16. Y. Y. Wang, N. V. Wheeler, F. Couny, P. J. Roberts, and F. Benabid, "Low loss broadband transmission in hypocycloid-core Kagome hollow-core photonic crystal fiber," Opt. Lett. **36**(5), 669–671 (2011).
17. B. Debord, M. Alharbi, T. Bradley, C. Fourcade-Dutin, Y. Y. Wang, L. Vincetti, F. Gérôme, and F. Benabid, "Hypocycloid-shaped hollow-core photonic crystal fiber Part I: arc curvature effect on confinement loss," Opt. Express **21**(23), 28597–28608 (2013).
18. B. Debord, A. Amsanpally, M. Chafer, A. Baz, M. Maurel, J. M. Blondy, E. Hugonnot, F. Scol, L. Vincetti, F. Gérôme, and F. Benabid, "Ultralow transmission loss in inhibited-coupling guiding hollow fibers," Optica **4**(2), 209–217 (2017).
19. Z. Wang, W. Belardi, F. Yu, W. J. Wadsworth, and J. C. Knight, "Efficient diode-pumped mid-infrared emission from acetylene-filled hollow-core fiber," Opt. Express **22**(18), 21872–21878 (2014).
20. N. Dadashzadeh, M. Thirugnanasambandam, K. Weerasinghe, B. Debord, M. Chafer, F. Gérôme, F. Benabid, B. Washburn, and K. Corwin, "Power-scaling a Mid-IR OPA-pumped Acetylene-filled hollow-core photonic crystal fiber laser," in *Conference on Lasers and Electro-Optics*, OSA Technical Digest (2016) (Optical Society of America, 2016), paper STh4O.1.
21. P. B. Chapple, "Beam Waist and M^2 measurement using a finite slit," Opt. Eng. **33**(7), 2461–2466 (1994).
22. ISO Standard 11146, "Lasers and laser-related equipment – Test methods for laser beam widths, divergence angles and beam propagation ratios" (2005).
23. T. Y. Fan, "Laser Beam Combining for High-Power, High-Radiance Sources," IEEE J. Sel. Top. Quantum Electron. **11**(3), 567–577 (2005).
24. B. Chann, R. K. Huang, L. J. Missaggia, C. T. Harris, Z. L. Liau, A. K. Goyal, J. P. Donnelly, T. Y. Fan, A. Sanchez-Rubio, and G. W. Turner, "Near-diffraction-limited diode laser arrays by wavelength beam combining," Opt. Lett. **30**(16), 2104–2106 (2005).
25. V. A. Serebryakov, É. V. Boĭko, N. N. Petrishchev, and A. V. Yan, "Medical applications of mid-IR lasers. Problems and prospects," J. Opt. Technol. **77**(1), 6–17 (2010).
26. L. Vincetti, "Empirical formulas for calculating loss in hollow core tube lattice fibers," Opt. Express **24**(10), 10313–10325 (2016).
27. W. C. Swann and S. L. Gilbert, "Pressure-induced shift and broadening of 1510-1540 nm acetylene wavelength calibration lines," J. Opt. Soc. Am. B **17**(7), 1263–1270 (2000).

1. Introduction

Hollow-core Optical Fiber Gas Lasers (HOFGLAS) offer the high average power, high damage threshold and very good slope efficiency of gas lasers [1–5] along with the merits of a fiber-based laser [6]. The first successful demonstration of HOFGLAS by Jones *et al.* [7,8] heralded a new era in gas and fiber laser research. Since then, scientists have demonstrated HOFGLAS in a variety of gasses including HCN, CO_2 and I_2 [8–12], spanning a wide wavelength range, and even demonstrating CW operation [12,13]. Much of this success is owed to a new branch of hollow-core photonic crystal fibers (HC-PCF) based on an inhibited coupling (IC) mechanism [14,15]; with the introduction of a hypocycloidal (*i.e.* negative curvature) core contour [16], record-setting propagation losses of 17 dB/km around 1 μm [17] and 7.7 dB/km at 750 nm [18] have been demonstrated. Such fibers have formed the basis of efficient HOFGLAS systems.

Acetylene-filled HOFGLAS is of specific interest because it can operate in the eye-safe mid-IR spectral region at 3 μm. It has a large scope for applications in remote sensing, communications, trace gas sensing and molecular fingerprinting. The lasing mechanism in acetylene that brings about stimulated emission at 3 μm has already been well discussed [5,9]. An improved realization of acetylene HOFGLAS by Jones *et al.* was reported [9,11] in which an optical parametric amplifier (OPA) pumped an acetylene-filled HOFGLAS that achieved laser operation at 3 μm with more than 20% slope efficiency. Recently, improved performance at 3 μm has also been demonstrated using a modulated, fiber-amplified diode laser as the pump laser [19]. Hassan *et al.* [13] added a feedback fiber to the traditional HOFGLAS system, thereby reducing the pump power required to produce 3 μm output.

Our work here highlights the power scalability and beam quality that can be achieved from a stable OPA-pumped acetylene-filled HOFGLAS configuration. We report the highest 3 μm pulse energy output achieved from an acetylene-filled pulsed HOFGLAS [20]. With a

Optics EXPRESS

HOFGLAS system comprised of a 10.9 m length of IC kagome fiber filled with acetylene at 9.8 torr, we were able to achieve the maximum 3 μm pulse energy of 1.4 μJ when acetylene absorbed 8.2 μJ of OPA pump pulse energy along the P(13) absorption line at 1.53 μm. To the best of our knowledge, this output laser pulse energy is nearly two times higher than the pulse energy reported in the most recent work [19]. The performance of the laser in terms of the highest 3 μm pulse energy that it can deliver is expected to increase further once higher pump pulse energies are employed. Also, the laser operated at a nearly constant slope efficiency of ~20% with respect to the absorbed pump pulse energy, nearly independent of the acetylene pressure inside the fiber.

The beam quality of the laser output was characterized using the finite slit method described in [21,22] to measure the beam waist along the focus and thereby obtain the M squared (M^2) of the 3-μm laser output. This first-time investigation of the beam quality of the output from acetylene-filled HOFGLAS yields M^2 of 1.15 ± 0.02 for the 3-μm output beam reflecting the near-diffraction limited performance of the laser. Given that beam combining results with M^2 of ~1.3 have been considered nearly ideal [23,24], the measured M^2 of our HOFGLAS system makes it an excellent candidate for coherent beam combining. The good beam quality also makes it a promising laser source when it comes to other applications in machining, medicine and telecommunications [23–25].

2. Experimental setup

The OPA-pumped acetylene-filled HOFGLAS setup is shown in Fig. 1(a). The key component of the setup is the 10.9 m long IC kagome-structured fiber. The low loss of the kagome-structured fibers over broad bandwidths makes them a suitable choice for fiber gas lasers that require a long interaction length. The core of these IC kagome fibers is hypocycloidal, which enhances the coupling inhibition between the core and cladding modes [16,17]. The fiber has an outer diameter of 360 μm and the hypocycloid core diameter varies between 60 μm and 72 μm, as shown in Fig. 1(c).

The design parameters of the fiber are chosen such that the fiber provides spatial guidance and bandwidth for the pump and lasing wavelengths, shown in Fig. 2(a), thereby enabling coherent laser emission. The fiber loss was measured to be 0.08 dB/m at the pump wavelength of 1.53 μm and 1.13 ± 0.05 dB/m at the average lasing wavelength of 3.1 μm. The measured loss is consistent with the empirical scaling laws reported in [26] for inhibited coupling HC-PCF.

The fiber is supported with its ends enclosed in vacuum chambers that can be filled with acetylene to required pressures (1.2 to 14 torr). The gas is allowed to reach equilibrium through the length of the fiber over a span of a few hours. The acetylene in the fiber is then pumped using an OPA that can produce a maximum pulse energy of 21 μJ with ~1 ns pulse duration, spectral width of 440 MHz based on the time-bandwidth product, and a repetition rate of 30 Hz at 1.53 μm. A combination of half-wave plate and polarizing beam splitter acts as a variable attenuator to regulate the pump pulse energy for the HOFGLAS setup. An anti-reflection (AR) coated BK7 lens is used to couple the pump pulse into the core of the fiber. An AR coated BK7 window on one of the vacuum chambers allows the pump to be coupled into the fiber and a CaF_2 window on the other chamber enables both the pump and laser wavelengths to be coupled out of the chamber efficiently.

The focal length of the lens that couples the OPA pump beam into the fiber is chosen such that the mode of the OPA pump beam has maximum overlap with the fundamental mode of the fiber. Improved mode quality of the homebuilt OPA output played a crucial role in obtaining a good energy coupling into the fiber. An average pump coupling efficiency of 52% was obtained from this configuration. The output beam is collimated using a CaF_2 lens of focal length 150 mm. A germanium filter at the output separates the laser output from the residual pump for laser diagnostics.

Optics EXPRESS

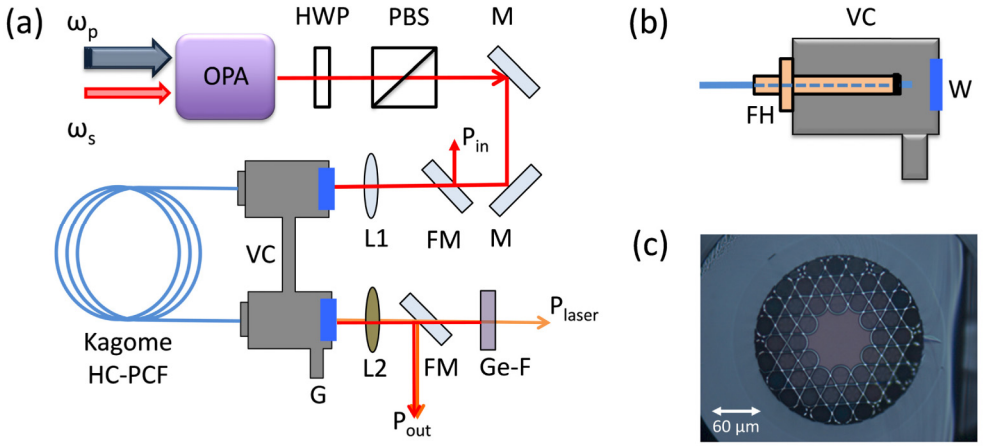

Fig. 1. (a) Schematic of C_2H_2 filled HOFGLAS pumped by an OPA operating at 1.5 µm, 30 Hz, 1 ns. The OPA is a MgO:PPLN crystal pumped by a Nd:YAG pulsed laser, ω_p, at 1.064 µm and seeded by a CW tunable fiber laser, ω_s, at 1.5 µm. HWP – Half wave plate, PBS – Polarizing beam splitter, M – Silver mirrors, FM – HR mirrors on flipper mount, L1- BK7 lens, L2 - CaF_2 lens, G – To gas inlet or roughing pump, VC - Vacuum chambers, P_{in} – Input OPA pump pulse energy, P_{out} – Output pulse energy, Ge-F – Germanium filter, P_{laser} – 3 µm output pulse energy. (b) Cross-section of vacuum chamber with fiber mounted using fiber holder. FH – Fiber holder, W- Window. (c) Cross-section of HC-PCF used in the laser setup showing the kagome lattice structure and the hypocycloidal core.

3. OPA pumped acetylene-filled HOFGLAS characteristics

The performance of the laser is characterized for various acetylene pressures in the fiber in terms of the spectral content of the laser output, the output pulse energy and laser beam quality, the results of which are discussed in the subsections that follow.

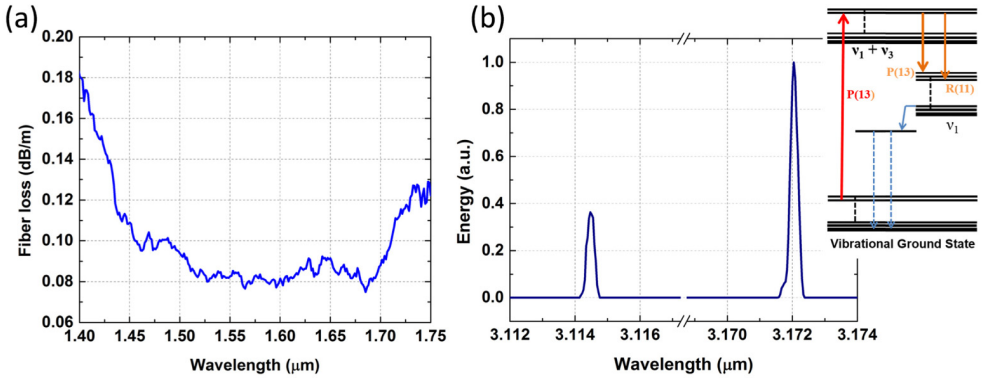

Fig. 2. (a) Measured loss in the IC kagome fiber around 1.5 µm pump wavelength region. (b) Spectrum of 3 µm output of acetylene HOFGLAS. Inset shows the simple molecular energy level diagram of acetylene. The lasing wavelengths are observed at 3.11 µm and 3.17 µm corresponding to the R(11) and P(13) transitions between the excited state $\nu_1 + \nu_3$ and the vibrational state ν_1.

The seed diode laser for the OPA allows tunability of the pump wavelength on and off resonance with the P(13) transition of acetylene at 1.53 µm. The seed laser for the OPA is tuned on resonance with the $\nu_1 + \nu_3$ P(13) transition line of acetylene. This results in laser emission along the P(13) and R(11) transitions.

Optics EXPRESS

3.1 Spectral content

The simple molecular structure of acetylene and the lasing transitions that lead to emission at 3 μm are shown in the inset of Fig. 2(b). To initiate lasing, the pump wavelength is tuned to the P(13) absorption line in acetylene, corresponding to the transition between the vibrational ground state and the $\nu_1 + \nu_3$ vibrationally excited state at 1.53 μm, which is Doppler-broadened to ~475 MHz and further pressure-broadened by ~11 MHz/torr [27]. Then population inversion between the rotational-vibrational states results in lasing at 3.11 μm and 3.17 μm which are the R(11) and P(13) lines in acetylene corresponding to the transitions between the excited state and the ν_1 vibrational state, as shown in Fig. 2(b).

3.2 Output pulse energy and laser efficiency

The use of sensitive pyroelectric energy meters allowed the characterization of the laser efficiency over a broad range of operating parameters. The 1.53 μm and 3 μm pulse energies were measured at different positions in the laser configuration. To measure pulse energy at 3 μm, a Ge filter placed just before the detector effectively blocked the residual 1.53 μm pump. Figure 3(a) shows the 3 μm output pulse energy as a function of the pump pulse energy coupled into the fiber when a coupling lens of focal length f = 75 mm was used. By measuring the input OPA pump pulse energy and the residual pump pulse energy after the vacuum chambers, it is possible to estimate the total pump pulse energy absorbed by the gas when the pulse is on resonance with the P(13) transition, distinct from of the pulse energy lost to imperfect fiber guidance or to imperfect coupling optics. The 3 μm output pulse energy from the laser versus the total pump pulse energy absorbed by acetylene in the fiber can hence be estimated for various acetylene pressures, Fig. 3(b).

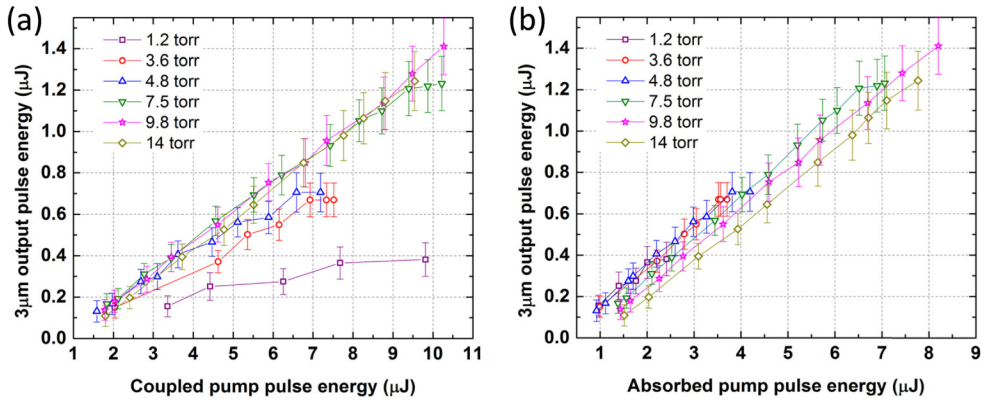

Fig. 3. Laser output pulse energy at 3 μm versus (a) coupled pump pulse energy at 1.53 μm into the fiber with coupling lens of focal length f = 75 mm, and (b) estimated pump pulse energy absorbed by gas. Error bars represent the standard deviation of individual pulses and are 9.7% at the maximum power.

A similar curve appearing in [20] shows slightly smaller quantities on the x-axis for estimated absorbed pump pulse energy. The discrepancy is due to a difference in the way the coupling efficiency was estimated when accounting for fiber loss. Figure 3 reflects our best understanding of those losses at the present time. It can be observed from Fig. 3 that for pressures below 9 torr, the 3 μm output energy increases but eventually saturates as the pump pulse energy absorbed by the acetylene gas increases. The saturated output pulse energies are plotted against the pressure of acetylene in Fig. 4(a). Also the slope efficiency of the laser is obtained by fitting the linear region of each curve in Fig. 3(b), and is plotted against acetylene pressure in Fig. 4(b) (purple squares).

Optics EXPRESS

For the range of pump pulse energy achievable from the current OPA, when acetylene pressure is above 9 torr the laser operates without seeing any saturation behavior, and produces a maximum 3 μm pulse energy of 1.41 μJ at 9.8 torr of acetylene pressure. At this highest output pulse energy, the slope efficiency of the laser is ~17% and the overall efficiency with respect to the incident pump pulse energy is ~14%. Figure 4(a) clearly shows that as the acetylene pressure increases, the pump energy at which saturation occurs increases. This may be due to linear dependence on pressure of the number of molecules participating in stimulated emission. The plot also shows the extrapolation of a linear fit to the measured values of saturated output pulse energies, suggesting that the output of the laser may reach 2 μJ without saturation when sufficient pump power can be realized. We expect this predicted power scaling at higher acetylene pressures provided that factors like pressure broadening, fiber loss, and other effects do not limit the laser performance at the higher pump powers.

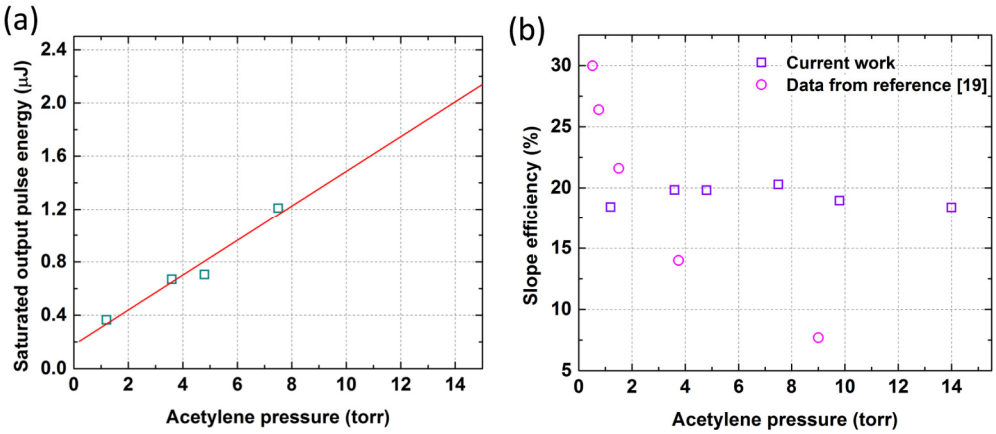

Fig. 4. (a) Saturated laser output pulse energy at 3 μm for various acetylene pressures. As acetylene pressure increases, the pump pulse energy at which saturation is observed for 3 μm output also increases. The red line shows the linear fit to the data with an extrapolation to higher pump pulse energies. (b) The laser slope efficiency for various acetylene pressures from Fig. 4(b) (purple squares) and reference [19] (magenta circles) are compared. The slope efficiency of the laser presented in the current work stays fairly consistent at ~20%.

We have also compared our laser efficiency with that of a diode pumped HOFGLAS configuration reported in [19], as shown in Fig. 4(b). It can be seen that while the laser efficiency of the diode-pumped configuration varies over a wide range from ~8% to ~30%, the slope efficiency of our OPA pumped HOFGLAS system stays fairly consistent and stable at ~20% over the same range of acetylene pressures for which the laser performance was investigated. The slope efficiency of the laser is nearly independent of the pressure of acetylene in the hollow core fiber, indicating that collisional relaxation is not a limitation on laser performance in this regime. This behavior is encouraging for scaling to higher pressures and pump powers. Further investigations are underway to understand the dependence of slope efficiency on the fiber loss at 3 μm and the length of the fiber.

3.3 M^2 of 3 μm output beam

The laser mode quality is characterized in terms of M^2, which provides information about the beam's propagation properties and achievable brightness. The M^2 is determined by measuring the beam profiles of the 3 μm laser output through the focus of a fixed position lens in free space when the laser operated at an acetylene pressure of 10 torr and coupling between the fiber and the 1.53 μm pump beam was optimized for single mode operation. In this case, 1.15 μJ was the maximum observed 3 μm pulse energy.

Optics EXPRESS

The beam widths reported here were measured using a CaF_2 plano-convex lens of 150 mm focal length and a 20-μm wide slit. The slit was scanned along the transverse axis (x) of the output beam to obtain beam profiles at different positions along the propagation axis (z). An example of this data set is shown in Fig. 5, for which a series of beam profiles was measured at the highest 3-μm pulse energy produced by the laser. This method of measuring the M^2 of the beam by scanning the beam using a slit at various axial positions typically requires a few hours owing to the 30 Hz repetition rate of our OPA pump in the current laser configuration. The laser operated stably through the measurement, which can be seen in the smoothness of the curves comprising the cascade plot of Fig. 5 and the small error bars in Fig. 3.

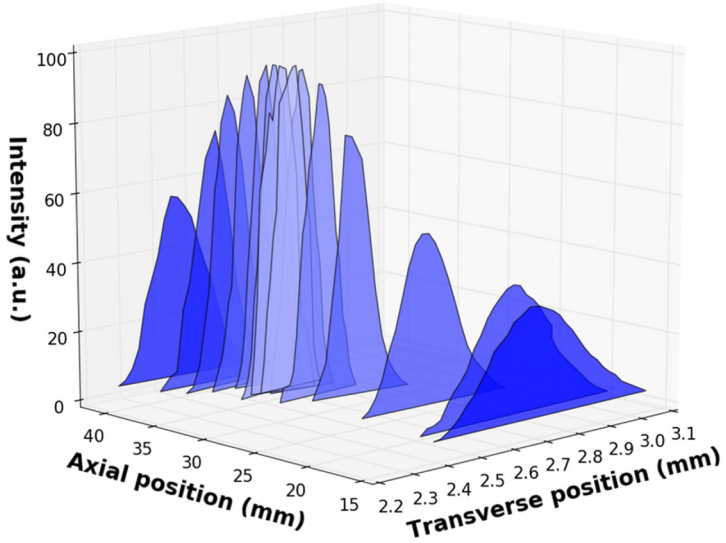

Fig. 5. The 3 μm laser beam profiles measured along the focus of a lens to determine the M^2 of the laser. The curves were measured when the laser was delivering the pulse energy of 1.15 μJ.

To extract M^2, the beam widths for each profile in Fig. 5 were obtained using the ISO standard D4σ method and were fitted to the definition of M^2 [21,22] with an averaged wavelength of 3.143 μm. Figure 6(a) shows beam widths calculated as the second moment of each beam profile curve in Fig. 5, and the fit that yields an M^2 value of 1.15 ± 0.02. The error in the M^2 value comes from fitting the measured beam widths to the definition of M^2 in [21], and represents the uncertainty on an average of 50 shots. The uncertainty on a measurement of individual pulses, assuming random noise, is expected to be ~0.14.

The M^2 of the laser output was also measured for other pump pulse energies when the HOFGLAS operated with acetylene pressure at 10 torr. The M^2 measurements at other pulse energies, shown in Fig. 6(b), indicate that the beam quality of the laser output stayed relatively uncompromised.

Optics EXPRESS

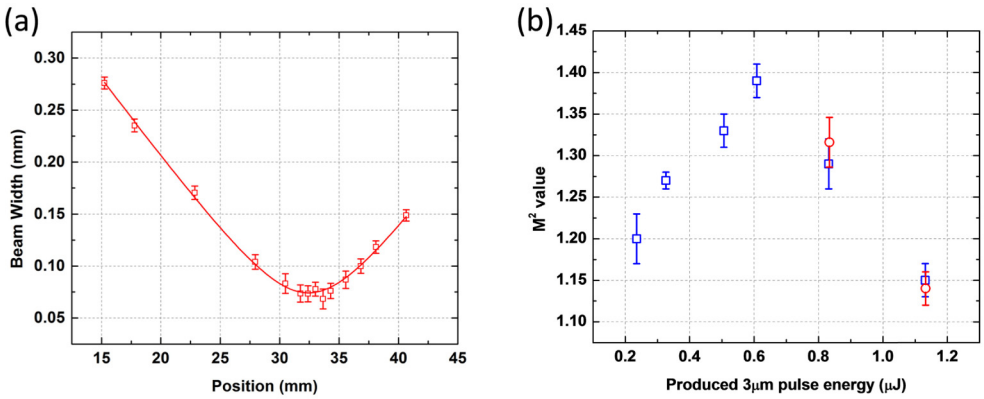

Fig. 6. (a) The beam width of the laser output measured using a 20 μm slit with HOFGLAS operating at highest pulse energy. Error bars represent fluctuations in the averages of 50 shots. The Gaussian fit for the beam width shows that the focal point lies at axial position 32.42 mm. (b) Measured M^2 values for the laser operating under acetylene pressure of 10 torr at various 3 μm output pulse energies; reproduced data points are shown in red.

M^2 measurement reproducibility was checked at two powers using a 50 μm wide slit. In both cases, M^2 values were reproduced as shown in Fig. 6(b). This shows the near-Gaussian beam profile of the produced 3μm output and hence the near-diffraction limited performance of the acetylene-filled HOFGLAS system. This clearly indicates that the laser operates stably with a good diffraction-limited beam quality.

4. Summary

We have demonstrated near-diffraction limited performance of an OPA-pumped acetylene-filled HOFGLAS system at high pulse energy near 3.1 μm. The HOFGLAS with a kagome-structured fiber and a hypocycloidal core of 10.9 m operates without any saturation at a slope efficiency of ~20% up to pulse energy of 1.4 μJ. The stable 3 μm output comes with a good mode quality (M^2 = 1.15) and improved performance over the previous realizations of acetylene-filled HOFGLAS systems with higher pulse energies and reduced dependence of slope efficiency on pressure.

Funding

Air Force Office of Scientific Research (AFOSR) (FA9550-14-1-0024). Air Force Research Laboratory (AFRL) (FA9451-17-2-0011). Agence Nationale de la Recherche (ANR) (PHOTOSYNTH) and (Σ_LIM Labex Chaire). La région Limousin.

Acknowledgments

We thank Wolfgang Rudolph and Vasudevan Nampoothiri for useful discussions, and Sajed Hosseini-Zavareh and the staff of the James R. Macdonald laboratory for helpful technical contributions. We also thank the PLATINOM platform for the help in the fiber fabrication.